Translational Oncology 13 (2020) 100808

Contents lists available at ScienceDirect

Translational Oncology

journal homepage: www.elsevier.com/locate/tranon

Characteristics of Head and Neck Squamous Cell Carcinoma Cell Lines Reflect Human Tumor Biology Independent of Primary Etiologies and HPV Status

Thankam S. Nair [a], Trey B. Thomas [a], Lucy Yang [a], Bala Naveen Kakaraparthi [a], Anna C. Morris [a], Alanna M. Clark [a], Lora P. Campredon [b], Andrew F. Brouwer [b], Marisa C. Eisenberg [b,c], Rafael Meza [b], Thomas E. Carey [a,*]

[a] Department of Otolaryngology-Head & Neck Surgery, Michigan Medicine, University of Michigan, Ann Arbor, MI, US 48109
[b] Department of Epidemiology, School of Public Health, University of Michigan, Ann Arbor, MI 48109
[c] Department of Mathematics, University of Michigan, Ann Arbor, MI 48109

ARTICLE INFO

Article history:
Received 12 February 2020
Received in revised form 15 May 2020
Accepted 26 May 2020
Available online xxxx

ABSTRACT

Explanations for the differences in clinical outcomes in head and neck squamous cell carcinomas (HNSCCs) when compared by similar tumor location, stage, nodal status, human papillomavirus (HPV) status, and patient history remain elusive. Cell lines are an excellent tool of study for understanding the *in vitro* properties of cancers. However, HNSCC cell lines from progression-free and/or HPV-positive tumors are very rare. Here we studied HPV-positive and HPV-negative University of Michigan squamous cell carcinoma cell lines (2 HPV−, 2 HPV16+, 1 HPV18+) coming from donors with nonoropharyngeal sites and variant clinical outcomes. Cell morphology and proliferation were assessed, and immunofluorescence and Western blotting evaluated tumor biomarkers (TP53, RB1, p16, HPV E6 and E7, EGFR, Cyclin D1, Ki-67, and beta-catenin). Slow *in vitro* proliferation, long lag phase before exponential proliferation, lower maximal cell density, and higher wild-type TP53 expression were common to cell lines from patients who experienced long-term disease-free survival. In contrast, shorter lag phases, rapid proliferation, and high maximal cell density were observed in cell lines from patients who experienced aggressive tumor progression leading to death. Membrane-bound beta-catenin was present in all cell lines, but nuclear beta-catenin was associated with the more lethal cancers. In summary, the HNSCC cell lines present key characteristics, independent of primary etiologies and HPV infection, that mirror the behavior of the tumors from which they were derived.

Introduction

Head and neck cancers account for 3%-4% of all cancer in the United States [1]. Human head and neck cancer cell lines are valuable tools for basic research, and the University of Michigan squamous cell carcinoma (UM-SCC) cell lines have been widely used around the world [2,3]. We have established more than 120 human head and neck squamous cell carcinoma (HNSCC) cell lines from patients treated at the University of Michigan, including three that are human papillomavirus (HPV) positive [4–6]. The UM-SCC cell lines are representative of all anatomic sites in the head and neck region, with the most common being larynx, oral cavity, oropharynx, and hypopharynx.

In addition to the widely known risk factors of smoking and alcohol consumption, high-risk HPV (HPV+) has become an important etiologic factor in HNSCC and especially oropharyngeal squamous cell cancers (OPSCCs) [7]. HPV+ HNSCC mostly arise in the oropharynx but also occur in the larynx, nasopharynx, and oral cavity [8–11]. Three-year survival rates of 70% and more have been reported for patients with HPV-driven oropharyngeal tumors [12–15]. While HPV+ laryngeal cancers may have a survival advantage when other factors are taken into account [9], HPV+ tumors arising in the oral cavity do not share the survival advantage of HPV+ OPSCC [16,17]. Unfortunately, most HNSCC cell lines, even those that are HPV+, are from patients with progressive disease [6], whereas only a few cell lines are from patients who have prolonged progression-free survival after treatment. This raises the following question: Are there differences that can be identified in the cell lines from those cancers that progress and those that do not?

In this study, we selected two of our laryngeal-based cancer cell lines (one HPV+ and one HPV−) that are from rare long-term survivors and three of our oral cavity cell lines (two HPV+, one HPV−) from patients with rapid tumor progression. It should be noted that these cell lines were

* Address all correspondence to: Thomas E. Carey, PhD, University of Michigan - Michigan Medicine, 1150 West Medical Center Dr., Ann Arbor, MI 48109-5616.
E-mail address: careyte@umich.edu. (T.E. Carey).

http://dx.doi.org/10.1016/j.tranon.2020.100808

not derived from HPV + OPSCCs that typically respond well to treatment. Although our cell lines (UM-SCC-17A, -38, -47, -104, and -105) are widely used by other researchers, we are the first to compare the characteristics that distinguish HNSCC cell lines from patients who had prolonged disease-free survival (DFS) after treatment to those of cell lines from patients who experienced rapid progression after treatment. The cell lines were evaluated for growth patterns; proliferation rates; and expression of key tumor biomarkers including TP53, RB1, p16, E6, E7, epidermal growth factor receptor (EGFR), Cyclin D1, Ki-67, and total and active beta-catenin.

Methods

Cell Culture and Cell Lines

The UM-SCC cell lines were developed in our laboratory following written informed consent from the patients granting their permission to use excess tissue removed at the time of treatment for research studies, including the development of cell lines. To minimize the possibilities of genetic drift, cross contamination or selection of minor clones, established cell lines are genotyped and tested for mycoplasma and refrozen in barcoded cryovials each time the cells are removed from the freezer. This maintains batches of genotyped and mycoplasma negative cells at low passage numbers. For all experiments, all five UM-SCC cell lines were used at the lowest available passages. These studies were reviewed and approved by the University of Michigan Medical School Institutional Review Board over a period of 38 + years (current IRB HUM00042189). The cell lines selected for this study included UM-SCC-17A [18], UM-SCC-38 [19], UM-SCC-47, UM-SCC-104, and UM-SCC-105 [6,20]. CaSki (HPV16 + cervical cancer) [21], HeLa (HPV18 + cervical cancer) [22], and HOK-16B (HPV16 + transformed normal human oral keratinocyte) [23,24] cell lines were used as controls and were generously provided by the originators, ensuring correct provenance. Additionally, all cell lines were genotyped using Profiler Plus (ThermoFisher.com) [5], and the genotype confirmed their identity.

Tumor cell lines were grown in complete Dulbecco's modified Eagle medium containing 2 mM L-glutamine, penicillin (100 U/ml), streptomycin (100 μg/ml) (Invitrogen), and 10% fetal bovine serum (Sigma-Aldrich). HOK-16B was grown in keratinocyte growth medium with supplements (Invitrogen). All cultured cells were incubated at 37°C in 5% CO_2 and room air. Mycoplasma tests were done routinely to rule out contamination using a MycoAlert kit (Lonza, Lonza.com/research).

Cell Proliferation

Cells in exponential growth were detached with trypsin (0.1% with 0.125% EDTA) (1:3 diluted trypsin solution was used to detach HOK-16B) and passed into plates or flasks to maintain exponential growth. For proliferation experiments, UM-SCC cell lines were plated in duplicate at 250,000 viable cells/well in six-well plates (9.5 cm^2) and counted every other day for 17 days. HOK-16B cells were plated at 40,000 cells/well in six-well plates. For biomarker expression by immunofluorescence, multiple six-well plates were prepared with coverslips and seeded with 250,000 cells/well from the same cell suspension used for proliferation. In addition, duplicate T-25 flasks were seeded with 500,000 cells/flask for protein harvests. For the cell growth experiments, the medium was changed every 3 days. Cells were harvested and resuspended in 100-500 μl media for counting with trypan blue to obtain viable cell counts. On the same days as the cell counts, coverslips were harvested and fixed, and flasks were harvested at each time point for protein isolation. HeLa and CaSki cells were not included in the cell proliferation studies but were used for comparative protein expression during midexponential growth.

Immunofluorescence and Western Blotting

Immunofluorescence (IF) assays were performed as previously described [25]. Cells grown on coverslips from multiple six-well plates were fixed with 2% formaldehyde and permeabilized with 0.2% Triton x-100.Primary antibodies were incubated for 2 hours, and after washing, secondary antibodies were incubated for 45 minutes at room temperature. Photomicrographs of IF staining were taken at the same gain for each antibody using the confocal or inverted phase contrast microscope equipped for fluorescence.

Primary antibodies included: TP53 clone DO-1 and RB1 clone Rb1 (ThermoFisher Scientific); CINtec-kit for p16, also called $p16^{INK4a}$ (clone E6H4 Roche Diagnostic); EGFR (anti-EGFR clone 31G7) (Invitrogen); Cyclin D1 (Santa Cruz Biotechnology); Ki-67 (Millipore/Sigma); anti–beta-catenin clone 14 (610,153 BD Biosciences); and monoclonal rabbit antibody to active (nonphosphorylated ser33/37/thr41) beta-catenin (D13A1 Cell Signaling). The antibodies to TP53 (clone DO-1) and RB1 (clone RB1) are specified by the manufacturer to bind well to both wild-type (WT) and mutant protein. Goat anti-mouse and goat anti-rabbit IgG heavy and light chain specific secondary antibodies, labeled with Alexa 546 (Invitrogen), were used to detect primary antibody binding. Light and confocal microscopy photographs were obtained.

Immunoprecipitation and Western blotting were carried out as previously described [26]. Cells plated at 500,000 cells/T-25 flask (for HOK-16B, 80,000 cells/T-25) were lysed and sonicated in RIPA buffer and kept frozen at −80°C. Protein concentrations were determined using the BCA (Pierce) assay. Western blots (WBs) were loaded with 25-50 μg of protein for each lane as noted. Blots were probed with the same anti-TP53, RB1, p16, EGFR, Cyclin D1, Ki-67, and beta-catenin antibodies as listed above. Prediluted antibodies to p16 and EGFR were further diluted to 1:10. Most antibodies were used at 1:100 to 1:1000. Beta-catenin clone 14 was used at 1:10,000. Anti-GAPDH (Santa Cruz Biotechnology) (diluted 1:3000) provided a control for protein loading.

Detection of E6 and E7 proteins is difficult. Therefore, we modified existing methods to increase our ability to detect the viral oncoproteins. These included increased protein loading, longer incubation times, and mixtures of antibodies to overcome the low affinities of individual antiviral oncoprotein antibodies. In WB experiments for E7, 50 μg protein/sample was used for SDS-PAGE. Transferred proteins were blocked with 5% milk for an hour followed by E7 antibodies (HPV16 E7 sc-65,711, HPV18 E7 sc-365,035, from Santa Cruz Biotechnology) with incubation at a dilution of 1:50 to 1:100 for 24 to 48 hours at 4°C or 1:100 and 1:500 for four nights at 4°C. For E6 protein detection, antibodies specific for HPV16/18 E6 (sc-460) and HPV18 E6 (sc-365089) from Santa Cruz Biotechnology were used. Since the abundance of E6 protein was low, it was first concentrated by immunoprecipitation with an antibody specific for HPV16/18 E6 conjugated to agarose beads. Cell extracts containing 300-500 μg of protein were mixed with 10 μl of agarose-coupled E6 antibody (HPV16 E6/18 E6 AC, sc-460AC, Santa Cruz Biotechnology) and rocked overnight at 4°C. Beads carrying the precipitated E6 protein were washed and boiled in nonreducing sample buffer. From briefly spun samples, the supernatants were saved and mixed with beta-mercaptoethanol for loading on SDS-PAGE gels. The immunoprecipitated E6 protein was blotted and probed with HPV16/18 E6-specific antibody and HPV18 E6-specific antibody mixed together and was incubated for three to five nights at 4°C.

For Western blotting, goat anti-mouse and anti-rabbit IgG heavy and light chain specific secondary antibodies conjugated to HRP (Jackson Immunochemicals) were used at 1:1000 to 1:2000, except for GAPDH where the secondary antibody was used at 1:20,000. Protein bands were visualized with an enhanced chemiluminescent reaction (GE Healthcare Life Sciences).

To better appreciate the differences in protein expression in the WBs for each of the cell lines, we used ImageJ to calculate semiquantitative values for biomarker expression taking into account the GAPDH loading control. Since E6 was immunoprecipitated, a loading control was not available. Therefore, the E6 blot was assessed for staining density per unit area of the band normalized to the staining density of the UM-SCC-105 E6 band from the early exponential growth phase set to 1.00.

Results

Cell Line Donor History

The donor of the UM-SCC-17A cell line (HPV−) [18] was a 48-year-old white female with a 40-pack-year history of cigarette smoking who developed a T1N0M0 cancer of the larynx that was treated initially by radiation (60 Gy). The tumor persisted and was restaged as T2N0M0. The patient underwent laryngectomy, and the UM-SCC-17A cell line was established from tumor within the larynx, although invasion through the laryngeal cartilage was present. This patient remained free of disease for at least 17 years before succumbing to a lung cancer that could have been a new primary tumor or an indolent metastasis from the laryngeal cancer (Table 1 summarizes the characteristics of each cell line, including donor history).

UM-SCC-38 (HPV−) [19] was developed from primary surgical treatment of a T2N2M0 cancer of the tonsillar fossa and base of tongue in a 60-year-old black male with an 80-pack-year history of cigarette smoking and 25 years of heavy alcohol use. The patient was treated with a partial tongue resection, radical neck dissection, and full-course radiation after surgery. The cell line was established from the tongue resection. His tumor recurred, and despite additional surgery and chemotherapy, he succumbed 11 months after his initial diagnosis and treatment.

UM-SCC-47 (HPV16+) [5,6] was established from a 53-year-old Hispanic male with an unknown but suspected smoking history who developed a T3N1M0 tumor of the lateral tongue. He was treated with a partial tongue resection, which provided tissue for the cell line, and radical neck dissection. He was referred for postoperative radiation at an outside hospital. His tumor progressed after treatment, and he died 7 months after diagnosis and surgical treatment.

UM-SCC-104 (HPV16+) [4] was established from a 56-year-old white male, with a history of 40 pack-years of cigarette smoking and 2 alcoholic drinks/day, who presented with a recurrent floor of mouth cancer as described previously [4,6]. After two surgeries plus chemotherapy and radiation, he was referred to the University of Michigan, where the persistent tumor was restaged as T4N2bM0. The floor of mouth and tongue tumor were resected, and tissue was sent to the laboratory for cell line establishment. The tumor progressed, and he succumbed 2 years after diagnosis.

UM-SCC-105 (HPV18+) [6] was established from the laryngectomy specimen of a nonsmoking, nondrinking 51-year-old white male with a T4N0M0 squamous cancer of the larynx who had been treated for a hoarse voice for more than a year until he suffered airway obstruction and was discovered to have a large tumor of the vocal cord. He was initially treated with TPF (Taxotere, 5FU, and carboplatin), but due to adverse reactions to the drugs, including neutropenia and electrolyte imbalances, he was referred to the University of Michigan and treated with a total laryngectomy and postoperative radiation therapy (RT). He remains alive with no evidence of disease more than 7 years after diagnosis.

Cell Proliferation

The growth pattern and morphology of the cells in culture are shown in Figure 1. The fastest-growing tumor cells, UM-SCC-38, -47, and -104, had short lag phases (3-5 days) before exponential growth and completed 4.25 population doublings within 11-13 days. Cell numbers decreased after reaching maximum cell density, probably due to competition for space and nutrients. Only UM-SCC-104 rebounded after such a decline in cell numbers. These three cell lines formed large islands that coalesced into monolayers rapidly, while UM-SCC-17A and -105 each had longer lag phases and tended to grow in smaller islands. The UM-SCC-17A islands increased in cell density without covering the entire surface of the culture vessel, whereas UM-SCC-105 islands consisted of large cells that slowly merged to form loosely packed low-density monolayers. HOK-16B grew rapidly as independent cells that were loosely attached to the substrate.

UM-SCC-17A required 17 days to complete slightly over 4 doublings (Figure 2; Table 1). UM-SCC-105 completed only 2.5 doublings over 13 days, and after maximal density of only 1.8×10^6 cells, UM-SCC-105 lost viable cells from day 13 to day 17. HOK-16B, which was plated at 4×10^4 cells per well, had a short lag phase, grew very rapidly, and underwent 5.5 doublings, reaching maximal cell density of 1.9×10^6 cells in 9 days. After that point, many cells detached from the plate surface and were replaced by rapidly growing cells repopulating the open space and reaching a new high density of 2.3×10^6 cells on day 17 (Figure 2).

Immunofluorescence

Proliferating cells were tested for expression of Ki-67 (*MKI67*), TP53 (*TP53*), p16 (*CDKN2A*), total beta-catenin (*CTNNB1*), and active beta-catenin using IF (Figure 3). For Ki-67, TP53, and p16, the strongest protein staining was observed by IF during exponential growth prior to reaching higher density. The photos in Figure 3 were taken between days 5 and 9. Photomicrographs of these same markers during earlier (days 1-3) and later (days 15-18) days of the proliferation experiments are shown in sFigure 1 and 2, respectively. The nuclear proliferation marker Ki-67 (Figure 3*A*) was highly expressed in all cell lines during the midexponential growth phase, and its expression tended to decrease as proliferation slowed at high cell density (sFigure 2*A*). TP53 protein expression was high only in HPV− UM-SCC-38, the only cell line with mutant *TP53*. The remaining cell lines contained WT *TP53* and showed very weak fluorescence (Figure 3*B*).

Table 1
Cell Line Characteristics, *TP53* Genotype, HPV Status, Growth Characteristics, Tumor Site and Stage, and Patient Survival

Cell Line	HPV Status	Lag Phase (Hours)	Start of Exponential Proliferation (Day)	Max Cell Density (Day)	Primary Site and Stage	Alcohol and Smoking History	Survival from Time of Diagnosis
UM-SCC-17A	HPV-	216	9	4.5 million [17]	Larynx T1N0M0; persistence after radiation	Nondrinker; 40 pack-years of smoking	17 years*
UM-SCC-38	HPV-	84	3.5	5.5 million [13]	Tonsillar pillar T2N2M0	25 years of heavy alcohol use; 80 pack-years of smoking	11 months DOD
UM-SCC-47	HPV16+	84	3.5	4.9 million [13]	Lateral tongue T3N1M0	Alcohol use unknown; suspected tobacco use	7 months DOD
UM-SCC-104	HPV16+	120	5	5 million [11]	Primary site unknown; recurrence floor of mouth	2 alcohol drinks/day; 40 pack-years of smoking	2 years DOD
UM-SCC-105	HPV18+	276	11.5	1.8 million [13]	Larynx T4N0M0	No alcohol use reported; nonsmoker	>7 years NED
HOK-16B	HPV16+	72	3	1.9 million [9]; 2.3 million [17]	Human oral keratinocytes	N/A	N/A

HPV status was determined by the multiplex HPV PCR MassArray assay [4,6]. Expression of HPV16 E6 and E7 was confirmed by RT-PCR of cDNA from the HOK-16B cell line. Lag phase is defined as the proliferation rate after plating until the inflection point when exponential proliferation begins (see Figure 2). Start of exponential proliferation is taken as the day that the growth curves change slope from the lag phase. Primary site and stage: Primary site is the site of the original diagnosis of head and neck squamous cancer, and staging is from first diagnosis. UM-SCC-17A and UM-SCC-104 were established from recurrent or persistent tumors after first treatment. *DOD*, died of disease; *NED*, no evidence of disease (alive).

* Donor of UM-SCC-17A died of a lung neoplasm, possible new primary cancer, or metastasis from the original larynx cancer.

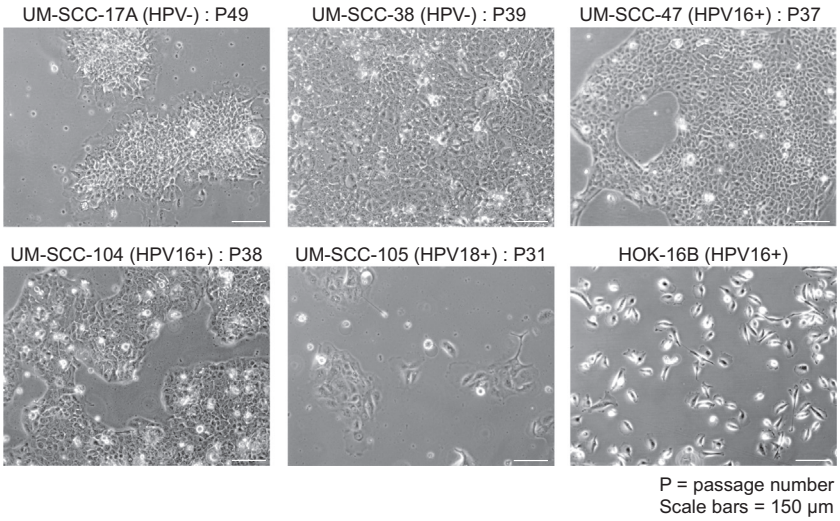

Figure 1. Phase contrast micrographs of cell lines from the exponential growth phase. Representative images taken during the exponential growth phase for each cell line including the passage number of the cells used in the study. *In vitro* passage number for HOK-16B is unknown. Phase contrast microscopy at 100× magnification. Scale bars = 150 µm.

IF expression of p16 was absent in the HPV− cell lines, weak in UM-SCC-47, and stronger in UM-SCC-104 and -105 and HOK-16B (Figure 3*C*). We compared the expression of total (Figure 3*D*) and active (nonphosphorylated) beta-catenin (Figure 3*E*) using antibodies reported to distinguish the active form from membrane-bound beta-catenin. For each cell line, the total and active beta-catenin showed membrane staining in all cell lines. However, in UM-SCC-38, -104, and to a lesser extent in -47, nuclear staining was present.

Western Blots

WB experiments were performed to better characterize the levels of key protein biomarkers, TP53, RB1, p16, HPV E6 and E7, EGFR, Cyclin D1, Ki-67, total beta-catenin, and active beta-catenin, using cell extracts from cells in midexponential growth (Figure 4). TP53 protein was most strongly expressed in UM-SCC-38. Lower levels of expression were observed in UM-SCC-17A, UM-SCC-105, HeLa, and CaSki. UM-SCC-47 and -104 displayed very little TP53 (Figure 4*A*). RB1 was highly expressed in UM-SCC-104, HeLa, and CaSki; lower in UM-SCC-17A, -38, and -105; and lowest in UM-SCC-47 (Figure 4*B*). p16 protein was expressed by all HPV+ cell lines, with lower expression in UM-SCC-47 and HeLa (Figure 4*C*).

HPV E6 and E7 were expressed exclusively in the HPV+ cell lines. E6 expression varied with time from plating such that it was barely detectable on days 5 or 6 in UM-SCC-47, -104, and -105 but became stronger on days 9 and 10 (Figure 4*D*, note asterisk on later dates). E6 expression in UM-SCC-47 and CaSki was barely detectable regardless of sample date (Figure 4*D*). E6 protein in the CaSki cell line was difficult to detect when exposed together with the other cell lines. Longer exposure revealed that the E6 protein was present but at lower abundance. In contrast, E7 was strongly expressed in UM-SCC-47, UM-SCC-104, and CaSki. In HPV18+ UM-SCC-105 and HeLa, E7 expression was less pronounced and migrated at a lower molecular mass than the HPV16 E7 protein (Figure 4*E*).

The cell lines reflected variability in EGFR expression with high expression in UM-SCC-17A, -38, -104, and -105 and low expression in UM-SCC-

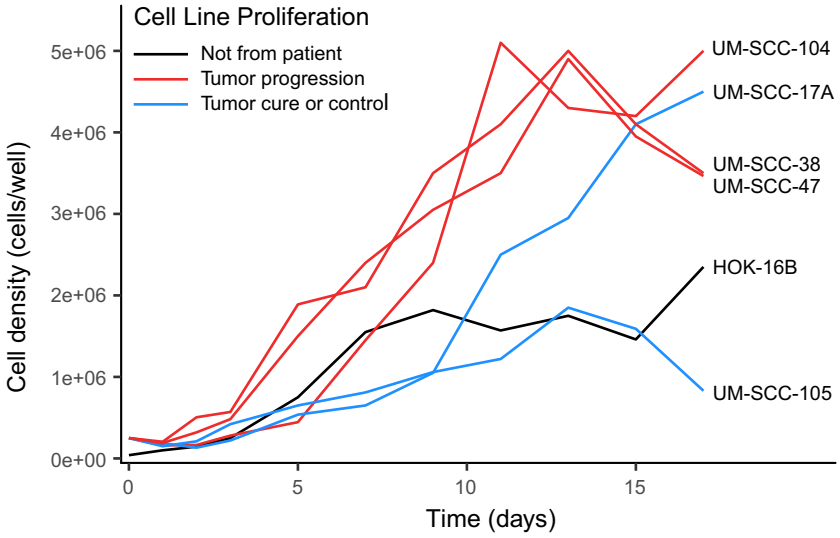

Figure 2. Composite cell growth curves for all cell lines. Growth dynamics show strong early (i.e., short lag phase after plating) growth to reach high maximal cell density (~5 × 10^6 cells/well) within 11-13 days in UM-SCC-38, -47, and - 104 (red lines). In contrast, UM-SCC-17A and - 105 (blue lines) exhibited a prolonged lag phase of slow proliferation prior to reaching exponential growth starting on day 9 and 11, respectively. HOK-16B control cells (black line) exhibited early rapid doubling, reaching 1.9 × 10^6 cells/well on day 9, after which the cells sloughed off the plate before resuming rapid proliferation on day 15.

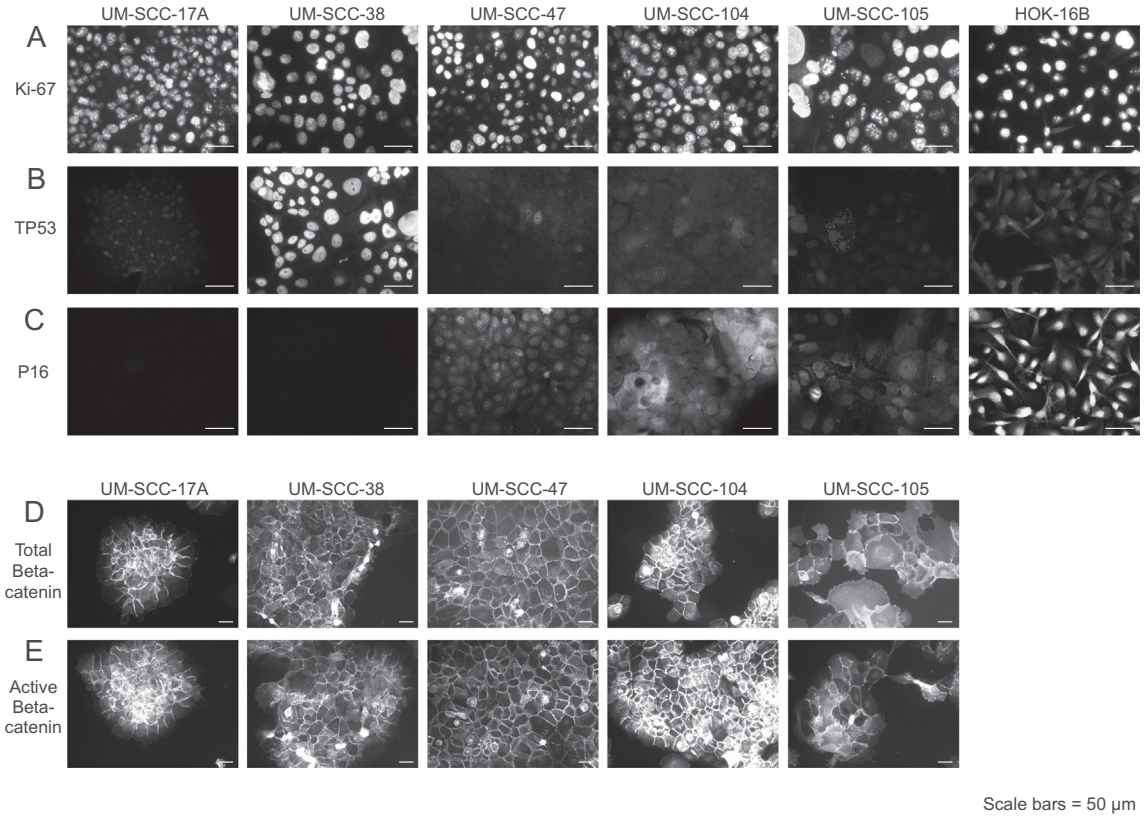

Figure 3. Immunofluorescence microscopy of protein biomarkers. Ki-67 (A), TP53 (B), p16 (C), total beta-catenin (D), and active beta-catenin (E) in all cell lines during exponential growth phases. Cells were at roughly 70% confluence. Photomicrographs were taken during days 5-9 with an inverted light microscope equipped for fluorescence. Scale bars = 50 μm.

47, HeLa, and CaSki (Figure 4*F*). Cyclin D1 expression was most strongly expressed in UM-SCC-38 and to a lesser extent in UM-SCC-104, UM-SCC-105, HeLa, and CaSki. Low-level expression was detectable in UM-SCC-17A and -47. All of the cell lines, except CaSki, strongly expressed high–molecular weight Ki-67. Smears of degraded protein were present in most extracts but to a much lower degree in UM-SCC-47 and -104. UM-SCC-105 and HeLa, the two highest-expressing lines, had the most degradation. Only a lightly stained smear of degraded Ki-67 was observed in CaSki (Figure 4*H*). Total beta-catenin expression was similar in UM-SCC-17A, UM-SCC-38, UM-SCC-47, UM-SCC-104, and CaSki, with lesser amounts in UM-SCC-105 and barely detectable expression in HeLa (Figure 4*I*). A similar distribution was seen in active beta-catenin expression (Figure 4*J*). The lower level of beta-catenin expression in UM-SCC-105 was consistent with its less intense IF staining (Figure 3*D*). The semiquantitative analysis of biomarker expression supported these visual descriptions (Tables 2A and 2B).

Genetic Analyses

To better understand the variations in protein expression among the cell lines, we examined the genetic analyses that have been performed on the UM-SCC cell lines used in this study [2,20]. A summary of the status of *TP53, TP63, CDKN2A, RB1, ERBB1, CCND1*, and *CTNNB1* is shown in Table 3. Expression of TP53 matched the genetic analysis of the five cell lines. All cell lines contain WT *TP53*, except for UM-SCC-38, which has a homozygous missense mutation of *TP53* consistent with its protein overexpression. We did not show expression of TP63 protein, but it is included in Table 3 since *TP63* is altered by an HPV16 E6*1 ≥ E7 ≥ E1 insertion into intron 11, with *TP63* exon 14 reading into E5 of HPV16 [6]. The integrated region is amplified, which may influence the level of HPV16 E6 expression in UM-SCC-47. Curiously, only UM-SCC-17A has two WT copies of *TP63*. *TP63* is amplified by copy gain of chromosome 3q in all of the HPV+ lines, but in UM-SCC-38, there is a truncating mutation of one copy together with amplification of the other copy of *TP63*. *CDKN2A* is deleted in UM-SCC-38, which is consistent with the absence of expression of p16. UM-SCC-47 is hemizygous for *CDKN2A,* which may account for the reduced expression of p16. All cell lines are WT for *RB1* except for UM-SCC-104, which has a frameshift deletion. EGFR expression did not correlate with the genetic status of the cell lines. All UM-SCC cell lines have WT *ERBB1,* and except for UM-SCC-17A, all have copy number gain and express EGFR more strongly than the cervical cancer cell lines. Similarly, the genetic status of *CCND1* does not correlate with Cyclin D1 expression. UM-SCC-38 had the highest expression of Cyclin D1 despite having loss of heterozygosity at this locus. *CTNNB1* is WT in all cell lines, though UM-SCC-105 exhibited lower total and active beta-catenin.

Discussion

The poor response to therapy in some HNSCCs, including nonresponsive HPV+ tumors, is not fully understood. Major risk factors, such as tobacco and alcohol use [27–30], can worsen treatment response and decrease survival rates [14,31–33]. Expression of viral-host fusions may also predict poor outcomes in HPV+ OPSCCs [6,34,35]. Of the HNSCC cell lines that we studied, three (two HPV+, one HPV−) were from the oral cavity, and all three oral cavity tumors progressed rapidly despite two having HPV infection and all three receiving aggressive treatment. In contrast, the donors of UM-SCC-17A and -105 had laryngeal cancers and experienced prolonged survival after treatment. It could be argued that the cartilaginous boundary of the larynx acts as a barrier to cancer spread and provided an advantage to the survival of these patients. However, the donor of UM-SCC-17A experienced progression after RT and had erosion through the laryngeal cartilage into the soft tissues of the neck, indicating that the cartilaginous boundary had been violated [18]. Furthermore, despite having a history of extensive tobacco use and extralaryngeal extension, the donor of UM-SCC-17A still experienced a 17-year disease-free

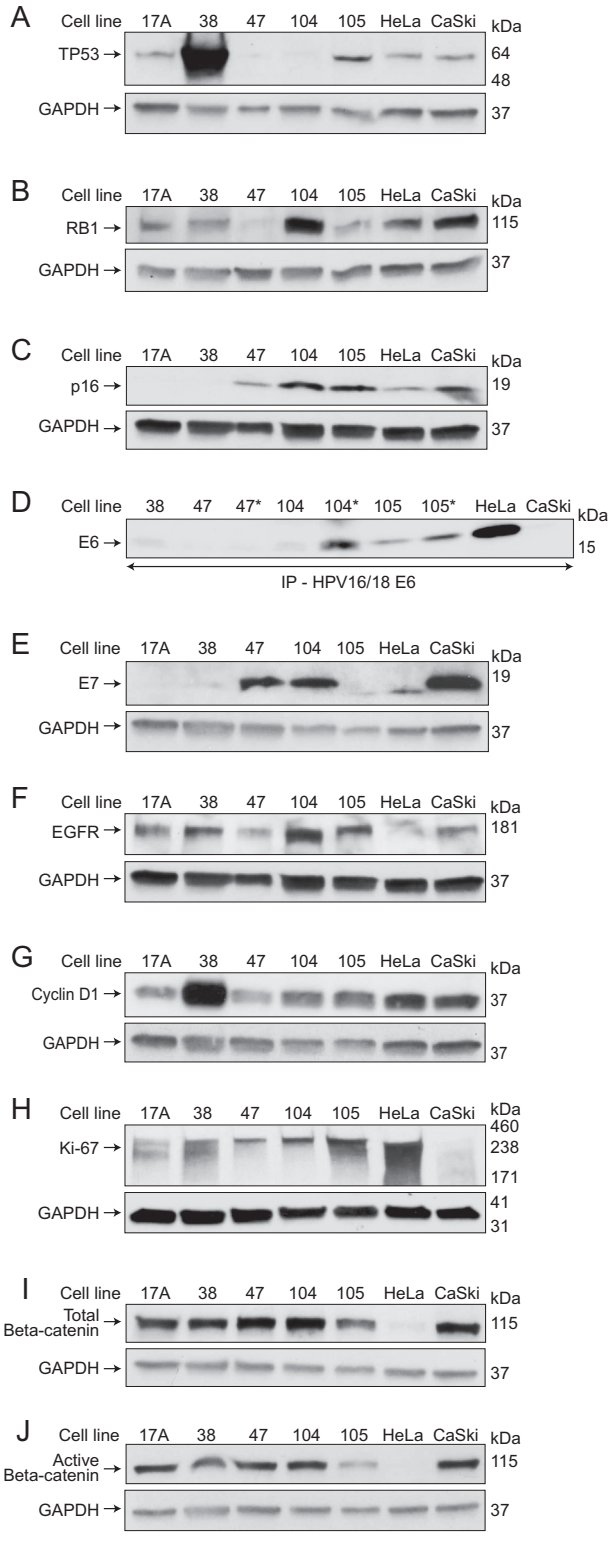

Figure 4. Biomarker expression by Western blotting during exponential growth phase. TP53 (A), RB1 (B), p16 (C), E6 (D), E7 (E), EGFR (F), Cyclin D1 (G), Ki-67 (H), total beta-catenin (I), and active beta-catenin (J). Protein was loaded at 50 μg per lane for all biomarkers except for total beta-catenin and active beta-catenin, which were loaded with 25 μg of protein. GAPDH was included as a loading control. (C and F) The same GAPDH staining was used since p16 and EGFR were probed from the same blot. (D) E6 was the only protein that was immunoprecipitated prior to WB due to its weaker expression. As a result, it was not possible to show a loading control. E6 was probed both in early (days 5-6) and later exponential growth phase (days 9-10, indicated by *). (G) Cyclin D1 staining was stripped to detect GAPDH.

interval after surgery [36]. The tumor in the donor of UM-SCC-105 may have been contained within the larynx, though the patient did receive surgery and full-course postoperative RT. Unlike the oral cavity tumor patients that donated UM-SCC-38, -47, and -104 and failed surgery +/− RT, it is reasonable to assert that the two patients with laryngeal cancers had less biologically aggressive tumors *in vivo*. Therefore, in this study, we analyzed these five cell lines for *in vitro* differences beyond HPV status or their primary etiologies that correlate with donor outcome.

The cell morphology (Figure 1) provided conflicting clues to biological behavior. UM-SCC-17A had a tendency after passage to proliferate in a stratifying manner to form tight colonies without migrating cells and formation of confluent monolayers. This might suggest a low propensity for migration and metastatic behavior. UM-SCC-38, -47, and -104, derived from aggressive tumors, formed large colonies that eventually fused to cover the entire culture surface, but this growth pattern alone does not provide clues to *in vivo* behavior. However, their very rapid doubling time compared to UM-SCC-17A and UM-SCC-105 does.

Proliferation analysis (Figure 2) of the cell lines reflected the aggressiveness of the tumors from which they were derived. UM-SCC-38, -47, and -104 grew rapidly with steep slopes, especially during the exponential growth phase. UM-SCC-17A exhibited a long lag phase of slower doubling time before the exponential growth phase, as did UM-SCC-105. Altogether, rapid entry into exponential *in vitro* proliferation, higher maximal doubling time, and shorter time to maximal density of the cell lines roughly correlate with the *in vivo* behavior of the corresponding tumors.

Biomarkers previously linked to cancer outcomes were examined by immunofluorescence and Western blotting for differences in protein expression across the cell lines. Immunofluorescent staining was best suited only to early phases of proliferation since staining for multiple markers became obscured with increasing confluence and multilayering of the cells.

Ki-67 protein is associated with actively cycling cells and has been reported as a controversial marker of rapidly proliferating tumors and improved response to chemotherapy, particularly in breast cancer [37–39]. During the midexponential growth phase, all cell lines in our study had strong IF expression of Ki-67 that corresponded to the abundant high–molecular weight protein observed in WB. However, Ki-67 did not distinguish the behavior of the cell lines from each other.

TP53 staining was high only in UM-SCC-38, consistent with its mutant *TP53*. In general, when *TP53* is mutated, the protein tends to be overexpressed and accumulates in tumor cells since the mutant forms are less effectively degraded. The HPV+ cell lines, as well as UM-SCC-17A, showed lower TP53 expression since they contain the WT gene. These patterns in the HPV+ cells are consistent with E6-induced ubiquitination of TP53 and its export from the nucleus in HPV+ cells [40]. However, the degree to which this degradation takes place in the HPV+ cell lines is difficult to determine, especially since the level of E6 protein was relatively low and barely detectable, except in UM-SCC-104 and HeLa. This may reflect the high level of alternate splicing of E6 in these cell lines which have very low full-length E6 transcripts but abundant E6*I and E6*II transcripts [6]. The alternate transcripts lack the codons required for the critical amino acids involved in E6 dimerization necessary to recruit E6AP to TP53 for ubiquitination, nuclear export, and degradation [41,42]. Comparatively higher WT TP53 was common to UM-SCC-17A and UM-SCC-105, suggesting that perhaps tumors with stronger WT TP53 expression are more responsive to treatment, as the donors of these cells lines had the best clinical outcomes.

As expected, only the HNSCC HPV+ cell lines expressed E6 and E7. The canonical E7-RB1 interaction [43] can explain the low RB1 expression in HPV+ tumors. Both HPV16+ cell lines, UM-SCC-47 and -104, had strong E7 expression. UM-SCC-104, contains a frameshift mutation of *RB1*.The mutant RB1 protein expression was high indicating that the mutation did not interfere with its transcription and translation. The functional nature of the frameshift mutation is unknown, but the strong protein expression suggests that the mutation affects the E7-binding pocket. If the mutation adversely affects the E7 binding pocket that would impair the ability of E7 to sequester the RB1 protein resulting in high RB1 expression. Similarly, if the

Table 2A
Semiquantitative Analysis of Biomarker Expression Relative to GAPDH

	UM-SCC-17A	UM-SCC-38	UM-SCC-47	UM-SCC-104	UM-SCC-105	HeLa	CaSki
TP53	1.00	15.02	0.16	0.07	2.76	0.80	0.90
RB1	1.00	0.90	0.15	3.11	0.56	1.22	2.13
p16	0.04	0.05	1.00	2.63	2.76	0.81	2.57
E7	0.02	0.08	3.62	6.17	1.00	1.44	5.11
EGFR	1.00	1.24	0.64	1.76	1.18	0.46	0.94
Cyclin D1	1.00	5.30	0.93	2.38	2.89	2.53	2.04
Ki-67	1.00	1.76	0.79	0.99	3.21	4.53	0.62
Total beta-catenin	1.00	0.96	1.12	1.62	0.84	0.03	1.15
Active beta-catenin	1.00	0.78	0.90	1.20	0.35	0.03	1.19

All semiquantitative biomarker comparisons except for p16 and E7 used UM-SCC-17A as the reference cell line. The p16 and E7 expressions in UM-SCC-17A were either too weak or absent to serve as a meaningful comparison. Instead, the HNSCC cell lines with the next lowest detectable p16 and E7 expressions were selected, which were UM-SCC-47 and UM-SCC-105, respectively.

Table 2B
Semiquantitative Analysis of E6 Biomarker Expression

	UM-SCC-38	UM-SCC-47	UM-SCC-47*	UM-SCC-104	UM-SCC-104*	UM-SCC-105	UM-SCC-105*	HeLa	CaSki
E6	0.35	0.23	0.26	0.52	4.42	1.00	2.32	9.14	0.18

UM-SCC-105 during the early exponential growth phase was selected as the reference cell line for the semiquantitative comparison for E6 because it had the lowest detectable E6 expression that could serve as a meaningful comparison.

* Later exponential growth phase.

mutation alters the binding pocket it would also inhibit E2F-binding leading to continuos activation of E2F-mediated expression of cell cycle entry genes. This would contribute to the aggressive growth of the tumor in the UM-SCC-104 donor. Curiously, UM-SCC-105 and HeLa, both HPV18+, expressed E7 less strongly than the HPV16+ cell lines, which may be due to poorer binding of the HPV18 E7 antibody. The HPV18-related E7 protein also migrated at a lower apparent molecular mass than the E7 protein from HPV16+ cell lines. The explanation for this is not known but suggests that HPV18 E7 protein may have a more compact tertiary molecular structure that migrates more rapidly in the in the gel.

Only the HPV+ cell lines expressed p16, which is consistent with actively expressed E7 binding to and sequestering RB1, thereby releasing E2F to continuously drive expression of cell cycle genes and p16 expression. UM-SCC-47 expressed p16 protein weakly as measured by both IF and WB. As *E7* message [6] and E7 protein were both strongly expressed in UM-SCC-47, the failure of stronger p16 expression in this cell line could be due to partial *CDKN2A* loss, mutation, or methylation [44–48], which is common in HPV− cancers [49] but rare in HPV+ cancers [17]. In fact, Cheng et al. [20] reported haploinsufficiency of CDKN2A in UM-SCC-47 (Table 3), which can explain the weak p16 expression in this cell line. UM-SCC-104 expressed p16 strongly, which is consistent with the hypothesis that the frameshift mutation of *RB1* inhibits E2F sequestration in this cell line. The basis for strong p16 expression in UM-SCC-105 is less clear. The strong p16 expression in UM-SCC-105 was accompanied by low E7 expression, but in spite of weak E7 expression, RB1 was also very low. The absence of strong RB1 expression may leave E2F available to drive early gene and p16 expression in UM-SCC-105. We noted that E7 expression was poorly identified by the E7 antibody in the HPV18+ HeLa cells as well as in UM-SCC-105. Thus, the apparently low E7 expression could be the result of weak antibody binding to HPV18 E7 protein, and the HPV18 E7 protein may be very effective in sequestering RB1, irrespective of the WB results. Superior outcomes in non-OPSCC, determined to be p16+ by *in situ* hybridization, and presumed to be HPV positive, have been reported in three large Radiation Therapy Oncology Group studies [17]. However, HPV status and p16 expression level alone are not necessarily predictive for survival in individual cases as we observed for the donors of these cell lines.

While EGFR has been implicated as a biomarker of aggressive squamous cell carcinomas [30], it is expressed in most HNSCC tumor specimens [50]. All of the HNSCC cell lines displayed strong EGFR expression, except for UM-SCC-47. Undetectable to minimal expression was seen in the cervical cancer cell lines HeLa and CaSki. Clinical studies have shown value in targeting EGFR as an adjunct to radiotherapy, primarily in the treatment of tonsil cancers [51]. However, the level of EGFR expression did not predict response when anti-EGFR treatment was added to radiotherapy with cisplatin in p16+ HNSCC [51,52]. Cyclin D1 has also been described as a marker of aggressive HNSCCs that is also associated with improved response to cisplatin chemotherapy [53,54]. Among the HNSCC cell lines, only UM-SCC-38 had strong expression of Cyclin D1, but the cell line

Table 3
Genetic Analyses

Gene	UM-SCC-17A	UM-SCC-38	UM-SCC-47	UM-SCC-104	UM-SCC-105
TP53	WT/WT	Homozygous missense G396T	WT/WT	WT/WT	WT/WT
TP63	WT/WT*	Truncating Mut/AMP	HPV16 integ/AMP	AMP WT/WT	AMP WT/WT
CDKN2A	WT/WT	Homozygous deletion	WT/−	WT/WT	WT/WT
RB1	WT/WT	WT/WT	WT/WT	Frameshift deletion	WT/WT
ERBB1	WT/WT*	WT copy number gain	WT copy number gain	WT copy number gain	WT copy number gain
CCND1	WT/WT*	WT/−	WT/−	WT/WT	WT/−
CTNNB1	WT/WT*	WT/WT*	WT/WT	WT/WT	WT/WT

Data from Cheng et al. (UM-SCC-38, UM-SCC-47, UM-SCC-104, UM-SCC-105) [20] and Nisa et al. (UM-SCC-17A) [2]. Sequencing of *TP53* in HOK-16B was not performed, but it is assumed to be WT. *AMP*, gene amplification. WT/− indicates a single copy loss. *TP63* is located on chromosome3q. In UM-SCC-104 and UM-SCC-105, 3q was present in multiple copies. In UM-SCC-47, HPV16 E6 ≥ E7 ≥ E1 is integrated into *TP63*, and the integrated region is amplified about nine-fold [3,6].

* WT confirmed but heterozygosity not reported.

donor of UM-SCC-38 was not treated with chemotherapy. Thus, these markers did not distinguish differences in the cell lines as compared to the *in vivo* behavior in the patients.

Active beta-catenin participates in the canonical Wnt signaling pathway, leading to nuclear translocation, if it is not phosphorylated and degraded by the catenin destruction pathway [55]. Strong total and active beta-catenin expression was observed in WBs, except in UM-SCC-105 and HeLa. However, what may be more important is where the beta-catenin is localized. As assessed by IF, UM-SCC-17A and -105 both had primarily membrane-bound beta-catenin, whereas UM-SCC-38, -47, and -104 exhibited more nuclear beta-catenin. Membrane-bound beta-catenin is transcriptionally silent, whereas nuclear beta-catenin acts as a cofactor for TCF/LEF transcription factors that drive the expression of genes involved in cell proliferation [56]. Higher nuclear beta-catenin localization is consistent with increased beta-catenin–driven transcriptional activity and more aggressive nature of the UM-SCC-38, -47 and -104 tumors. Similarly, absence of nuclear beta-catenin in UM-SCC-17A and -105 correlates with the better outcome in those patients' tumors.

Other studies have reported clinical associations with cell line development and biomarker expression in colon [57,58] and pancreatic [59] cancer cell lines, but those largely reflect the fact that most cancer cell lines are established from clinically aggressive tumors. A study from the University of Pittsburgh [60] investigated the success rate of HNSCC cell line establishment from 185 subjects, which resulted in 52 cell lines from 48 subjects. They found that tumors with 11q13 amplification and/or lymph node involvement were more likely to lead to successful cell line establishment. Additionally, the median observed survival time was 22 months if the tumor yielded a cell line and 60 months if it did not. If a tumor resulted in a cell line, the median DFS was 10 months, and if it did not, the median DFS was 37 months. Thus, it is clear that the establishment of an HNSCC cell line was a poor prognostic indicator. These studies reinforce the premise of this manuscript that tumor cell lines from long-term survivors are rare and that direct comparisons of the characteristics of cell lines that distinguish those from rapidly progressive tumors and those from long-term survivors are important areas for investigation.

The strength of this study is the comparison of cell lines from long-term survivors with similar cell lines from patients with aggressive cancers in a comprehensive analysis of cell growth and biomarker expression in well-characterized HPV− and HPV+ head and neck cancer cell lines. Protein expression was tested by immunofluorescence and Western blotting during the proliferation phase. The results demonstrated an advantage of Western blotting with respect to detection sensitivity and the ability to assess relative protein expression. However, for protein localization, as with beta-catenin, IF is more informative. Analysis of the genomic studies perfomed on the cell lines helped to explain differences in biomarker expression, which in turn helped to explain how these differences might correlate with outcome in the donor patients.

This study was limited by the relatively small number of cell lines from long-term survivors that are available for testing; nevertheless, we believe that our data will be beneficial to those who use these cell lines in thier research. It will be of interest to expand analysis of *in vitro* growth patterns, level of WT *TP53* expression, and nuclear beta-catenin expression to more cell line models to further test that these observations are factors that can relate to clinical behavior.

Conclusions

Low maximal cell density, long lag phase, and slow growth in cell proliferation, as well as higher expression of WT TP53 and lower expression of nuclear beta-catenin, were common to the cell lines derived from the HNSCC patients that experienced long-term DFS after definitive treatment. These results demonstrate that there are few key cell line characteristics that reflect the biologic behavior of these non-OPSCC tumors independent of primary etiologies and HPV status.

Supplementary data to this article can be found online at https://doi.org/10.1016/j.tranon.2020.100808.

Declaration of Competing Interest

None.

Funding

Grant support: National Institutes of Health National Cancer Institute U01 CA182915 (R.M., M.E., T.E.C.) and R01 CA194536 (T.E.C., J.C.B.).

References

[1] R.L. Siegel, K.D. Miller, A. Jemal, Cancer statistics, 2020, Ca-Cancer J Clin. 70 (1) (2020) 7–30.
[2] L. Nisa, D. Barras, M. Medova, D.M. Aebersold, M. Medo, M. Poliakova, et al., Comprehensive genomic profiling of patient-matched head and neck cancer cells: a preclinical pipeline for metastatic and recurrent disease, Mol. Cancer Res. 16 (12) (2018) 1912–1926.
[3] N.C. Olthof, C.U. Huebbers, J. Kolligs, M. Henfling, F.C. Ramaekers, I. Cornet, et al., Viral load, gene expression and mapping of viral integration sites in HPV16-associated HNSCC cell lines, Int. J. Cancer 136 (5) (2015) E207–E218.
[4] A.L. Tang, S.J. Hauff, J.H. Owen, M.P. Graham, M.J. Czerwinski, J.J. Park, et al., UM-SCC-104: a new human papillomavirus-16-positive cancer stem cell-containing head and neck squamous cell carcinoma cell line, Head Neck. 34 (10) (2012) 1480–1491.
[5] J.C. Brenner, M.P. Graham, B. Kumar, L.M. Saunders, R. Kupfer, R.H. Lyons, et al., Genotyping of 73 UM-SCC head and neck squamous cell carcinoma cell lines, Head Neck. 32 (4) (2010) 417–426.
[6] H.M. Walline, C.M. Goudsmit, J.B. McHugh, A.L. Tang, J.H. Owen, B.T. Teh, et al., Integration of high-risk human papillomavirus into cellular cancer-related genes in head and neck cancer cell lines, Head Neck. 39 (5) (2017) 840–852.
[7] A. Jemal, E.P. Simard, C. Dorell, A.M. Noone, L.E. Markowitz, B. Kohler, et al., Annual report to the nation on the status of cancer, 1975-2009, featuring the burden and trends in human papillomavirus (HPV)–associated cancers and HPV vaccination coverage levels, J. Natl. Cancer Inst. 105 (3) (2013) 175–201.
[8] J.H. Maxwell, B. Kumar, F.Y. Feng, J.B. McHugh, K.G. Cordell, A. Eisbruch, et al., HPV-positive/p16-positive/EBV-negative nasopharyngeal carcinoma in white North Americans, Head Neck. 32 (5) (2010) 562–567.
[9] A. Scheel, E. Bellile, J.B. McHugh, H.M. Walline, M.E. Prince, S. Urba, et al., Classification of TP53 mutations and HPV predict survival in advanced larynx cancer, Laryngoscope 126 (9) (2016) E292–E299.
[10] M.H. Stenmark, J.B. McHugh, M. Schipper, H.M. Walline, C. Komarck, F.Y. Feng, et al., Nonendemic HPV-positive nasopharyngeal carcinoma: association with poor prognosis, Int. J. Radiat. Oncol. Biol. Phys. 88 (3) (2014) 580–588.
[11] H.M. Walline, C. Komarck, J.B. McHugh, S.A. Byrd, M.E. Spector, S.J. Hauff, et al., High-risk human papillomavirus detection in oropharyngeal, nasopharyngeal, and oral cavity cancers: comparison of multiple methods, JAMA otolaryngology– head & neck surgery. 139 (12) (2013) 1320–1327.
[12] F.Y. Feng, H.M. Kim, T.H. Lyden, M.J. Haxer, F.P. Worden, M. Feng, et al., Intensity-modulated chemoradiotherapy aiming to reduce dysphagia in patients with oropharyngeal cancer: clinical and functional results, J. Clin. Oncol. 28 (16) (2010) 2732–2738.
[13] H. Quon, M.A. Cohen, K.T. Montone, A.F. Ziober, L.P. Wang, G.S. Weinstein, et al., Transoral robotic surgery and adjuvant therapy for oropharyngeal carcinomas and the influence of p16 INK4a on treatment outcomes, Laryngoscope 123 (3) (2013) 635–640.
[14] F.P. Worden, B. Kumar, J.S. Lee, G.T. Wolf, K.G. Cordell, J.M. Taylor, et al., Chemoselection as a strategy for organ preservation in advanced oropharynx cancer: response and survival positively associated with HPV16 copy number, J. Clin. Oncol. 26 (19) (2008) 3138–3146.
[15] B.H. Haughey, M.L. Hinni, J.R. Salassa, R.E. Hayden, D.G. Grant, J.T. Rich, et al., Transoral laser microsurgery as primary treatment for advanced-stage oropharyngeal cancer: a United States multicenter study, Head Neck. 33 (12) (2011) 1683–1694.
[16] S. Tian, J.M. Switchenko, J. Jhaveri, R.J. Cassidy, M.J. Ferris, R.H. Press, et al., Survival outcomes by HPV status in non-oropharyngeal head and neck cancers: A propensity score matched analysis of population level data, Journal of Clinical Oncology 36 (15_suppl) (2018) 6005.
[17] C.H. Chung, Q. Zhang, C.S. Kong, J. Harris, E.J. Fertig, P.M. Harari, et al., p16 protein expression and human papillomavirus status as prognostic biomarkers of nonoropharyngeal head and neck squamous cell carcinoma, J. Clin. Oncol. 32 (35) (2014) 3930–3938.
[18] T.E. Carey, D.L. Van Dyke, M.J. Worsham, C.R. Bradford, V.R. Babu, D.R. Schwartz, et al., Characterization of human laryngeal primary and metastatic squamous cell carcinoma cell lines UM-SCC-17A and UM-SCC-17B, Cancer Res. 49 (21) (1989) 6098–6107.
[19] D.L. Van Dyke, M.J. Worsham, M.S. Benninger, C.J. Krause, S.R. Baker, G.T. Wolf, et al., Recurrent cytogenetic abnormalities in squamous cell carcinomas of the head and neck region, Genes Chromosomes Cancer. 9 (3) (1994) 192–206.
[20] H. Cheng, X.P. Yang, H. Si, A.D. Saleh, W.M. Xiao, J. Coupar, et al., Genomic and transcriptomic characterization links cell lines with aggressive head and neck cancers, Cell Rep. 25 (5) (2018) 1332–1345.
[21] Patillo RA, Hussa R, Story, M.T., Ruskert, A.C.F., Shalaby, M.R., Mattingly, R.F. Tumor antigen and human chorionic gonadotropin in CaSki cells: a new epidermoid cervical carcinoma cell line. Science 1977;196:1456–7.
[22] G.O. Gey, W.D. Coffman, M.T. Kubicek, Tissue culture studies of the proliferative capacity of cervical carcinoma and normal epithelium, Cancer Res. 12 (1952) 264–265.

[23] S. Li, M. Kim, H.M. Cherrick, J. Doniger, N. Park, Sequential combined tumorigenic effect of HPV-16 and chemical carcinogens Carcinogenesis, 13 (11) (1992) 1981–1987.
[24] N.H. Park, B.M. Min, S.L. Li, M.Z. Huang, H.M. Cherick, J. Doniger, Immortalization of normal human oral keratinocytes with type 16 human papillomavirus, Carcinogenesis 12 (9) (1991) 1627–1631.
[25] P.K. Kommareddi, T.S. Nair, Y. Raphael, S.A. Telian, A.H. Kim, H.A. Arts, et al., Cochlin isoforms and their interaction with CTL2 (SLC44A2) in the inner ear, J. Assoc. Res. Otolaryngol. 8 (4) (2007) 435–446.
[26] P. Kommareddi, T. Nair, B.N. Kakaraparthi, M.M. Galano, D. Miller, I. Laczkovich, et al., Hair cell loss, spiral ganglion degeneration, and progressive sensorineural hearing loss in mice with targeted deletion of Slc44a2/Ctl2, J. Assoc. Res. Otolaryngol. 16 (2015) 695–712.
[27] K.K. Ang, J. Harris, R. Wheeler, R. Weber, D.I. Rosenthal, P.F. Nguyen-Tan, et al., Human papillomavirus and survival of patients with oropharyngeal cancer, N. Engl. J. Med. 363 (1) (2010) 24–35.
[28] C. Fakhry, M.L. Gillison, G. D'Souza, Tobacco use and oral HPV-16 infection, JAMA 312 (14) (2014) 1465–1467.
[29] J.H. Maxwell, B. Kumar, F.Y. Feng, F.P. Worden, J.S. Lee, A. Eisbruch, et al., Tobacco use in human papillomavirus-positive advanced oropharynx cancer patients related to increased risk of distant metastases and tumor recurrence, Clin. Cancer Res. 16 (4) (2010) 1226–1235.
[30] B. Kumar, K.G. Cordell, J.S. Lee, F.P. Worden, M.E. Prince, H.H. Tran, et al., EGFR, p16, HPV Titer, Bcl-xL and p53, sex, and smoking as indicators of response to therapy and survival in oropharyngeal cancer, J. Clin. Oncol. 26 (19) (2008) 3128–3137.
[31] M.L. Gillison, Human papillomavirus-associated head and neck cancer is a distinct epidemiologic, clinical, and molecular entity, Semin. Oncol. 31 (6) (2004) 744–754.
[32] D.J. Adelstein, J.A. Ridge, M.L. Gillison, A.K. Chaturvedi, G. D'Souza, P.E. Gravitt, et al., Head and neck squamous cell cancer and the human papillomavirus: summary of a National Cancer Institute State of the Science Meeting, November 9-10, 2008, Washington, D.C, Head Neck. 31 (11) (2009) 1393–1422.
[33] F.P. Worden, H. Ha, Controversies in the management of oropharynx cancer, J. Natl. Compr. Cancer Netw. 6 (7) (2008) 707–714.
[34] H.M. Walline, C.M. Komarck, J.B. McHugh, E.L. Bellile, J.C. Brenner, M.E. Prince, et al., Genomic integration of high-risk HPV alters gene expression in oropharyngeal squamous cell carcinoma, Mol. Cancer Res. 14 (10) (2016) 941–952.
[35] L.A. Koneva, Y. Zhang, S. Virani, P.B. Hall, J.B. McHugh, D.B. Chepeha, et al., HPV integration in HNSCC correlates with survival outcomes, immune respeonse signatures, and candidate drivers, Molecular Cancer Research 16 (2017) 90–102 December.
[36] S. Takabayashi, A. Hickson, T. Owaga, K.-Y. Jung, H. Mineta, Y. Ueda, et al., Loss of chromosome arm 18q with tumor progression in head and neck squamous cancer, Genes, Chromosomes & Cancer. 41 (2004) 145–154.
[37] B. Acs, V. Zambo, L. Vizkeleti, A.M. Szazs, L. Madaras, G. Szentmartoni, et al., Ki-67 as a controversial predictive and prognostic marker in breast cancer patients treated with neoadjuvant chemotherapy, Diagn. Pathol. 12 (2017) 1–12.
[38] J. Chatzkel, J.S. Lewis, J.C. Ley, T.M. Wildes, W. Thorstad, H. Gay, et al., Correlation of Ki-67 proliferative antigen expression and tumor response to induction chemotherapy containing cell cycle-specific agents in head and neck squamous cell carcinoma, Head & Neck Pathology. 11 (3) (2017) 338–345.
[39] M.M. Tao, S. Chen, X.Q. Zhang, Q. Zhou, Ki-67 labeling index is a predictive marker for a pathological complete response to neoadjuvant chemotherapy in breast cancer: a meta-analysis, Medicine 96 (51) (2017).
[40] C.H. Chung, M.L. Gillison, Human papillomavirus in head and neck cancer: its role in pathogenesis and clinical implications, Clin. Cancer Res. 15 (22) (2009) 6758–6762.
[41] Y. Nomine, M. Masson, S. Charbonnier, K. Zanier, T. Ristriani, F. Deryckere, et al., Structural and functional analysis of E6 oncoprotein: insights in the molecular pathways of human papillomavirus-mediated pathogenesis, Mol. Cell 21 (5) (2006) 665–678.
[42] K. Zanier, Y. Nomine, S. Charbonnier, C. Ruhlmann, P. Schultz, J. Schweizer, et al., Formation of well-defined soluble aggregates upon fusion to MBP is a generic property of E6 proteins from various human papillomavirus species, Protein Expr. Purif. 51 (1) (2007) 59–70.
[43] S.N. Boyer, D.E. Wazer, V. Band, E7 protein of human papilloma virus-16 induces degradation of retinoblastoma protein through the ubiquitin-proteasome pathway, Cancer Res. 56 (20) (1996) 4620–4624.
[44] S. Koscielny, R. Dahse, G. Ernst, F. von Eggeling, The prognostic relevance of p16 inactivation in head and neck cancer, ORL J. Otorhinolaryngol. Relat. Spec. 69 (1) (2007) 30–36.
[45] V.A. Papadimitrakopoulou, J. Izzo, L. Mao, J. Keck, D. Hamilton, D.M. Shin, et al., Cyclin D1 and p16 alterations in advanced premalignant lesions of the upper aerodigestive tract: role in response to chemoprevention and cancer development, Clin. Cancer Res. 7 (10) (2001) 3127–3134.
[46] S.A. Ahrendt, C.F. Eisenberger, L. Yip, A. Rashid, J.T. Chow, H.A. Pitt, et al., Chromosome 9p21 loss and p16 inactivation in primary sclerosing cholangitis-associated cholangiocarcinoma, J. Surg. Res. 84 (1) (1999) 88–93.
[47] P. Cairns, T.J. Polascik, Y. Eby, K. Tokino, J. Califano, A. Merlo, et al., Frequency of homozygous deletion at P16/Cdkn2 in primary human tumors, Nat. Genet. 11 (2) (1995) 210–212.
[48] Chuang A, Sidransky D, Califano J, Liegeois N. Aberrant methylation of tumor suppressor genes as potential molecular markers for cutaneous squamous cell carcinoma. J Am Acad Dermatol. 2010;62(3):Ab8-Ab.
[49] D. Wang, J.C. Grecula, R.A. Gahbauer, D.E. Schuller, K.R. Jatana, J.D. Biancamano, et al., p16 gene alterations in locally advanced squamous cell carcinoma of the head and neck, Oncol. Rep. 15 (2006) 661–665.
[50] S. Kalyankrishna, J.R. Grandis, Epidermal growth factor receptor biology in head and neck cancer, J. Clin. Oncol. 24 (17) (2006) 2666–2672.
[51] J.A. Bonner, P.M. Harari, J. Giralt, R.B. Cohen, C.U. Jones, R.K. Sur, et al., Radiotherapy plus cetuximab for locoregionally advanced head and neck cancer: 5-year survival data from a phase 3 randomised trial, and relation between cetuximab-induced rash and survival, Lancet Oncol. 11 (1) (2010) 21–28.
[52] K.K. Ang, Q. Zhang, D.I. Rosenthal, P.F. Nguyen-Tan, E.J. Sherman, R.S. Weber, et al., Randomized phase III trial of concurrent accelerated radiation plus cisplatin with or without cetuximab for stage III to IV head and neck carcinoma: RTOG 0522, J. Clin. Oncol. 32 (27) (2014) 2940–2950.
[53] J. Akervall, D.M. Kurnit, M. Adams, S. Zhu, S.G. Fisher, C.R. Bradford, et al., Overexpression of cyclin D1 correlates with sensitivity to cisplatin in squamous cell carcinoma cell lines of the head and neck, Acta Otolaryngol. 124 (7) (2004) 851–857.
[54] J. Akervall, E. Brun, M. Dictor, J. Wennerberg, Cyclin D1 overexpression versus response to induction chemotherapy in squamous cell carcinoma of the head and neck - Preliminary report, Acta Oncol. 40 (4) (2001) 505–511.
[55] B.T. MacDonald, K. Tamai, X. He, Wnt/B-catenin signaling: components, mechanisms, and diseases, Dev. Cell 17 (1) (2009) 9–26.
[56] M. Stenner, B. Yosef, C.U. Huebbers, S.F. Preuss, H.P. Dienes, E.J. Speel, et al., Nuclear translocation of beta-catenin and decreased expression of epithelial cadherin in human papillomavirus-positive tonsillar cancer: an early event in human papillomavirus-related tumour progression? Histopathology 58 (2011) 1117–1126.
[57] L. Cayrefourcq, T. Mazard, S. Joosse, J. Solassol, J. Ramos, E. Assenat, et al., Establishment and characterization of a cell line from human circulating colon cancer cells, Cancer Res. 75 (5) (2015) 892–901.
[58] C. Maletzki, S. Stier, U. Gruenert, M. Gock, C. Ostwald, F. Prall, et al., Establishment, characterization and chemosensitivity of three mismatch repair deficient cell lines from sporadic and inherited colorectal carcinomas, PLoS One 7 (12) (2012), e52485. .
[59] X. Du, K. He, Y. Huang, Z. Xu, M. Kong, J. Zhang, et al., Establishment of a novel human cell line retaining the characteristics of the original pancreatic adenocarcinoma, and evaluation of MEK as a therapeutic target, Int. J. Oncol. 56 (3) (2020) 761–771.
[60] J.S. White, J.L. Weissfeld, C.C. Ragin, K.M. Rossie, C.L. Martin, M. Shuster, et al., The influence of clinical and demographic risk factors on the establishment of head and neck squamous cell carcinoma cell lines, Oral Oncol. 43 (7) (2007) 701–712.